



HAL
open science

Effect of the Time Dependent Loading of Type IV Cylinders using a Multiscale Model

Martinus P. Widjaja, Marco Alves, Mark Mavrogordato, Sébastien Joannès,
Anthony R. Bunsell, Georg Mair, Alain Thionnet

► **To cite this version:**

Martinus P. Widjaja, Marco Alves, Mark Mavrogordato, Sébastien Joannès, Anthony R. Bunsell, et al.. Effect of the Time Dependent Loading of Type IV Cylinders using a Multiscale Model. ICSH 2019 - 8th International Conference on Hydrogen Safety, Sep 2019, Adelaide, Australia. hal-02315016

HAL Id: hal-02315016

<https://hal.science/hal-02315016>

Submitted on 14 Oct 2019

HAL is a multi-disciplinary open access archive for the deposit and dissemination of scientific research documents, whether they are published or not. The documents may come from teaching and research institutions in France or abroad, or from public or private research centers.

L'archive ouverte pluridisciplinaire **HAL**, est destinée au dépôt et à la diffusion de documents scientifiques de niveau recherche, publiés ou non, émanant des établissements d'enseignement et de recherche français ou étrangers, des laboratoires publics ou privés.

EFFECT OF THE TIME DEPENDENT LOADING OF TYPE IV CYLINDERS USING A MULTI-SCALE-MODEL

M.P. Widjaja^{1,4}, M. Alves², M. Mavrogordato³, S. Joannès⁴, A. Bunsell⁴, G. Mair¹ and A. Thionnet^{4,5,*}

¹ BAM Federal Institute for Materials Research and Testing, Berlin, 12203, Germany

² Department of Mechanical Engineering, South Kensington Campus, Imperial College, London SW7 2AZ, United Kingdom

³ μ -VIS X-Ray Imaging Centre, University of Southampton, Highfield, Southampton, SO17 1BJ, United Kingdom

⁴ MINES ParisTech, PSL - Research University, MAT - Centre des Matériaux, CNRS UMR 7633 BP 87, 91003 Evry cedex, France

⁵ Université de Bourgogne, Mirande, Dpt. IEM, BP 47870, Dijon, France

* Corresponding author (alain.thionnet@mines-paristech.fr)

Keywords: fibre break, multiscale model, time dependent load, type IV cylinders

ABSTRACT

The current requirements for composite cylinders are still based on an arbitrary approach derived from the behaviour of metal structures, that the designed burst pressure should be at least 2.5 times the maximum in-service pressure [1]. This could lead to an over-designed composite cylinder for which the weight saving would be less than optimum. Moreover, predicting the lifetime of composite cylinders is a challenging task due to their anisotropic characteristics. A federal research institute in Germany (BAM) has proposed a minimum load-cycle requirement that mitigates this issue by using a Monte-Carlo analysis of the burst test results [2-3]. To enrich this study, more experiments are required however they are normally limited by the necessity of long duration testing times (loading rate and number of cylinders) and the design (stacking sequence of the composite layer).

A multi-scale model incorporating the micromechanical behaviour of composite structures has been developed at Mines ParisTech. The model has shown similar behaviour to that of composite cylinders under different loading rates [4]. This indicates that the model could assist the Monte-Carlo analysis study. An evaluation of the multi-scale model therefore has been carried out to determine its limitations in predicting lifetimes of composite cylinders.

The evaluation starts with the comparison of burst pressures with type IV composite cylinders under different loading rates. A μ CT-Scan of a type IV cylinder has been carried out at the University of Southampton. The produced images were analysed using the Fast-Fourier Transform (FFT) technique to determine the configuration of the composite layers, which is required by the model. Finally, the time dependent effect studied, by using the multi scale model, has been described. In the long-term, this study can be used to conduct a parametric study for creating more efficient design of type IV cylinders.

1.0 INTRODUCTION

In the past the reduction of CO₂ emission and greenhouse gases was not a global issue that needed to be treated with such high importance. However, it is now clear that concrete actions must be taken to reduce the devastating effect of global warming. For instance, reducing the consumption of carbon-based fuel, i.e. coal, benzene and diesel. Therefore, today, the development of solar, wind and wave energy has gained popularity. Such development is also required in the transportation sector and the most interesting clean technology to be developed is the use of hydrogen and electric vehicles which produce zero emissions.

The way that the energy is stored raises safety issues. Hydrogen gas has to be highly pressurised (35-70 MPa) and held in a pressure vessel or cylinder. As the vessels need to be stored onboard the vehicles, a thorough study to ensure their reliability is of vital importance and needs to be understood before they are marketed. There are several types of pressure vessel that can be used but type IV cylinders consisting of a high density polyethylene (HDPE) liner over wound by carbon fibre composite has become of particular interest. The composite filaments are wound with different orientations and thicknesses to ensure the appropriate load-bearing capability of the cylinders. This leads to a high-performance lightweight structure particularly interesting for the transportation sector.

The keyword here is the composite structures that primarily carries the load from internal pressurisation. Carbon fibre reinforced plastic structures can fail by different types of degradation that must be first understood if their reliability is to be evaluated. Most importantly, the combination of the fibres and the resin materials making up the composite structure introduces behaviour which is intimately related to their physical interactions. This makes the study more complex as the behaviour described at the fibre-matrix scale must be also connected to the macroscopic scale of the cylinder.

A particular study on the microscopic scale of a carbon fibre composite was conducted in 2005 [5]. This study focused on a unidirectional composite subjected to tensile loads in the direction of the fibres. It has been found that during a monotonic loading case, the damaging process begins with random fibre breakages throughout the whole specimen, which eventually coalesce to form clusters of fibre breaks which lead to failure. The introduction of viscoelastic material properties of the resin into the model has shown that stress relaxation around individual fibre breaks induces further breaks even under constant loads. This has been shown to be responsible for time-dependent behaviour of composite structures.

The carbon fibre filament wound in the geodesic paths of the pressure vessels gives a similar failure behaviour to that of a unidirectional composite subjected in tensile loading in the fibre direction. These understandings have been validated with the slow burst test conducted by BAM which have also shown a time-dependent results. However, a solution must first be found before using the model to study large composite structures. A study of a reduced volume method has been conducted and shown that it is possible to reduce the number of elements used for the fibre break model that leads to the reduction of required computational time [6-7]. Every simulation described in this paper has been made possible, thanks to the proposed solution of a reduced volume method.

Conducting burst test requires a considerable financial investment as well as time and effort in terms of man-hours on behalf of the experienced technicians. The model could be the means of obtaining a much more efficient result. Therefore, a study has been carried out to ensure the capabilities of the fibre break multi scale model. After the performance of the model has been validated, the prediction from the model could then be used to improve the burst strength input data of the probabilistic approach from BAM. This tool has been developed to predict the lifetime of composite pressure vessels, which eventually leads to a critical suggestion for the existing standards.

2.0 METHODOLOGY

2.1 Parameter identification

The study began with the identification of the orientations and thicknesses of the composite layers making up the type IV pressure vessels (CPV) that have been burst-tested by BAM. The fibre volume fraction of the CPV is also an important parameter which needs to be known. These are the parameters that could play a major role on the accumulation of damage inside a composite pressure vessel, which eventually determines its burst strength. Therefore, accurate parameters are required for the model to have a comparable analysis with the experimental result. To achieve this, a collaboration with the University of Southampton has been carried out to conduct an investigation using the micro-CT machines. The general information of the CPV is described as follows,

- Working pressure : 30 MPa
- Volume : 6.8 L
- Total length : 565 mm
- Diameter : 165 mm

The concept of computed tomography (CT) scans has been initially developed for medical purposes. However, it has now become a popular non-intrusive technique to study composite materials, as identification and segmentation of damage processes has been made possible through this technique. An X-ray source was used to project a slice of the scanned object. This projection was then captured on a detector with the size of 2000 x 2000 pixels. As the object was rotated during the scans, all slices of the whole volume could be captured. The reconstructed volume could then be further analysed using the free imaging software FIJI ImageJ.

There are two parameters that must be identified to use the multiscale model for simulating CPV. Two machines have been used to obtain these parameters. The first machine has been used for capturing the stacking sequence of the CPV and the second one to get the fibre volume fraction of the hoop layer. To achieve the resolution that would give a favourable result on the first machine, a small cube specimen of about 6 mm x 6 mm x 6 mm has been extracted from the CPV with the aid of a water jet cutting machine. The resolution of the reconstructed 3D volumes was found to be ± 7 microns. On the other hand, the second machine required even smaller specimen. This has been done by extracting a matchstick specimen from the previously extracted cube. The resolution on this one achieved as great as 400 nanometres. This reconstructed 3D volume of such high resolution allowed the calculation of fibre volume fraction and the study of fibre-waviness to be carried out. The latter might also have an effect to the load redistribution process, which will not be discussed in this paper.

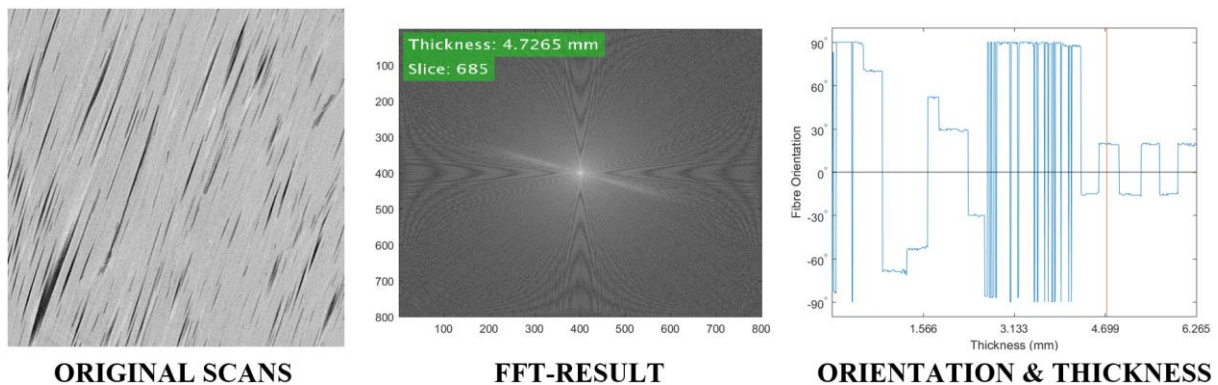


Figure 1. Post-processing images to determine the stacking sequence

The Fast-Fourier-Transform (FFT) technique has been used on the 3D reconstructed volume images from the first machine. The FFT function was applied for each slice of the volume, hence creating a new image, which allowed the most dominant attributes of the sliced images to be seen. In this case, this attribute would be the orientation of the composite layer. As the scans have been performed throughout the whole thickness of the composite layer, the position of each sliced image then could be calculated, as can be seen in Fig. 1. From this data, the average value of the orientation and the thickness for each layer then could be determined. The similar technique has also been used for measuring the fibre misalignment in unidirectional fibre composites [8].

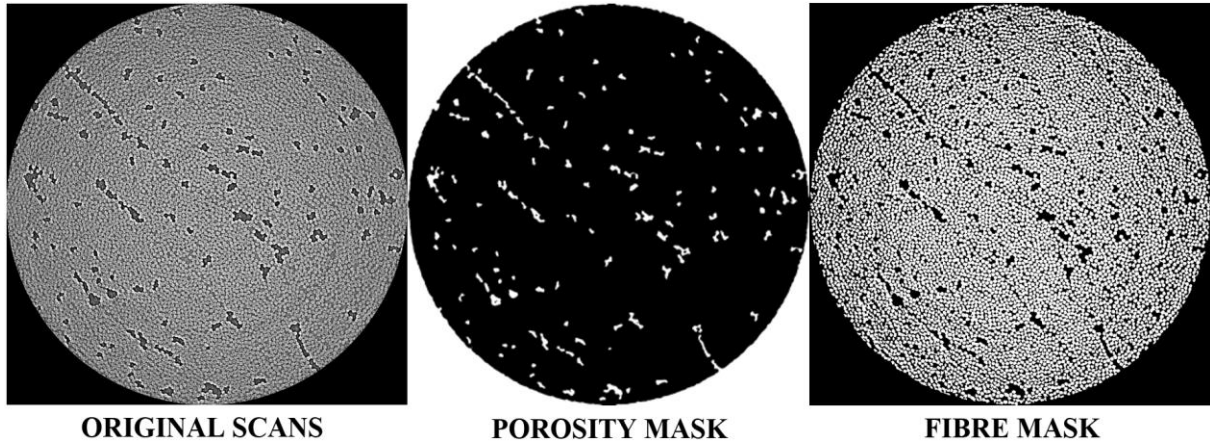


Figure 2. Post-processing images to determine fibre volume fraction

The resulting images from the second machine were used to determine the fibre volume fraction of the extracted hoop layer from a previously obtained cubic specimen. By using the FIJI-ImageJ software, segmentation between fibres and porosity became possible. First, a Gaussian blur function was used to capture the porosity region. This has been done by subtracting the original scans with the blurry mask. Secondly, by subtracting the original scans with the porosity mask, the fibre and matrix images could be obtained. Then, the combination of Gaussian blur and watershed function have been used to capture only the fibre regions. Even though, there is no general procedure to do this, qualitatively, the results are quite representative as can be seen in Fig. 2. In the end, the area fraction of the fibres can be measured at each slice of the images. The average values of the fibre area fraction were then calculated to be $59.92\% \pm 0.3$. The orientation, thickness, and fibre volume fraction information were then used as the input parameters for the fibre break model to simulate the CPV.

Table 1. Stacking sequence of the type IV pressure vessel and material assignment

LAYER	NUMBER	ORIENTATION ($^{\circ}$)	THICKNESS (mm)	MATERIAL MODEL
HOOP	1	89	0.5	FIBRE BREAK
OUTER HELICAL 1	2	70	0.3	LINEAR ELASTIC
OUTER HELICAL 2	3	-69	0.3	
OUTER HELICAL 3	4	-53	0.3	
OUTER HELICAL 3	5	52	0.3	
OUTER HELICAL 3	6	29	0.3	
OUTER HELICAL 3	7	-31	0.3	
HOOP	8	89	1.6	
INNER HELICAL 1	9	-15	0.3	LINEAR ELASTIC
INNER HELICAL 2	10	19	0.3	
INNER HELICAL 2	11	-16	0.3	
INNER HELICAL 2	12	19	0.3	
INNER HELICAL 3	13	-15	0.3	
INNER HELICAL 3	14	19	0.3	
LINER	15	-	2	LINEAR ELASTIC

Table 2. Comparison of composite material properties [9]

Composite	C₁₁ (MPa)	C₂₂ (MPa)	C₆₆ (MPa)	m	σ_0 (GPa)
T600S/epoxy [5]	149080	13974	5470	5.62	4.32
T700S/epoxy [10]	151090	11375	4500	4	5.8

The T600S composite material properties were those used for this study. Notice that the difference with the stiffness of T700S composite was not significant. However, the parameters of the Weibull distribution, which are the shape (m) and scale (σ_0) parameters were quite different. This would affect the accumulation process of the fibre breaks. The liner was modelled with an isotropic linear behaviour where its modulus and Poisson's ratio were 300 MPa and 0.4, respectively.

2.2 Fibre break model

The fibre break model has been implemented inside a simplified FE2 algorithm, which allows the relation between macro and microscale to be described [11]. In the microscale, the model explains the stochastic behaviour of fibre ruptures which can be described by two parameters Weibull function. Moreover, the effect of the debonding process between the fibre and the matrix that is induced by the broken fibre has also been integrated. More importantly, the matrix behaviour has been modelled as a viscoelastic material and this has allowed the stress relaxation process to be understood [12]. This relaxation process can cause a delayed fibre failure process which explains the time dependent behaviour of composite structures. The original study was conducted to define the required size of the element that can represent all those effects, which is 0.05 mm x 0.05 mm x 4 mm [13]. However, the stress field calculated using twice the size of the representative volume element (RVE) has been shown to give a similar result. Therefore, the composite structures must be modelled with the element size of 0.1 mm x 0.1 mm x 8 mm, which then contains 8 RVE [14]. The 3D element type with 6 degree of freedoms at each integration points is imperative to be used to capture the correct representation of the stress field.

The model since then has been improved to include the clustering process of fibre break in composite structures when they are subjected to tensile forces in the fibre direction [15]. Fig. 3 shows the development of damage states where i-plets have been broken incrementally explained by the damage states of C2, C4, C8, C16 and C32. Each of the damage states required one fibre strength value that has been described by the Weibull distribution. Therefore, 40 (8 RVE x 5 damage states) fibre strength values are required at each element of the modelled structure to conduct one simulation. When a new database of fibre strength values was used, a Monte-Carlo process then described the random nature of the fibre breaks throughout the entire volume of composite structures.

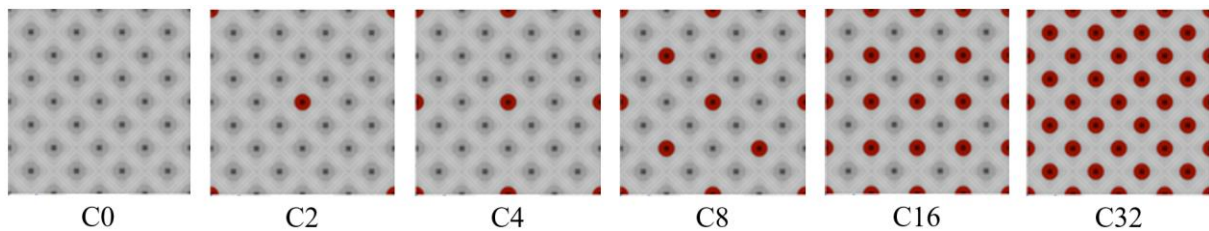


Figure 3. Different state of damage inside the fibre break model [15]

It is a simplified FE2 approach because only the calculated load transfer coefficients from the initial microstructural study that have been used for breaking the fibres. First, the calculated stress at each Gauss points was multiplied by the coefficient of load transfer between a broken fibre and neighbouring intact fibres. This value then will be compared with the calculated stress field at the macroscopic scale. If it was larger than the macroscopic stress, the fibre was deemed to be broken. With this approach, at each time step of FE calculation, the accumulation of damage could be studied. At each time step, the rigidity of the structure had also been updated and this could be done by using the equation below.

$$Q_{11} = Q_{11}^0 x (1 - 1/NFC), \quad (1)$$

Where Q_{11} is the updated stiffness of the material in the fibre direction, Q_{11}^0 is the current stiffness of the material in the fibre direction, and NFC is the number of fibres that are still undamaged in the structure [4].

2.3 Reduced volume method

When a large composite structure is modelled with the element size of 0.1 mm x 0.1 mm x 8 mm, the total number of the degree of freedoms that must be solved is incredibly large. A method that allows the 3D elements to be used and not necessarily change the failure prediction of the model must be investigated. As the input for the fibre break model is based on a two parameter Weibull distribution and requires multiple Monte-Carlo runs, there might be a way to obtain a similar prediction with fewer number of elements. The reduced volume method basically evaluates the prediction of strength from the model and showed that it is possible to do so. The reduced volume method has allowed a representative volume zone to be found, which eventually was able to determine the required number of Monte-Carlo simulations to attain certain relative error values [6-7]. However, in terms of modelling a CPV, it must be understood that the model must be deployed throughout the whole annular section because of the random nature of the fibre breaks. Further information can be found concerning the ergodic theory and integral range in references [16-19].

2.4 Simulation

The studied material system R characterised by the centre of the circle O with the length of L. The internal and external surfaces of the ring is described as S_{int} and S_{ext} . The ring is characterised by the r_{int} and r_{ext} and the total thickness of the wall was t_{tot} . These orientations in the model was described so that each element was defined with respect to the local coordinates of the ring. The dimensions of the ring were as follows: $L=0.01$ mm, $r_{int} = 74.8$ mm, $t_{tot} = 7.7$ mm. A uniform internal pressure P_{int} of 0.1667 MPa/s, 0.0025 MPa/s, and 0.00025 MPa/s, which was of the same loading rate that has been used for the experiment was then applied to the internal surface S_{int} as the boundary condition. The geometry had been constrained so that only displacement in the X and Y axes was allowed. Only elements in the hoop layer were made to approximately match the element size of the RVE (0.1 mm x 0.1 mm x 8mm). The rest of the layer was then described as 1 element per thickness as shown in Fig. 4. Such an approach has been taken based on the study of a reduced volume method.

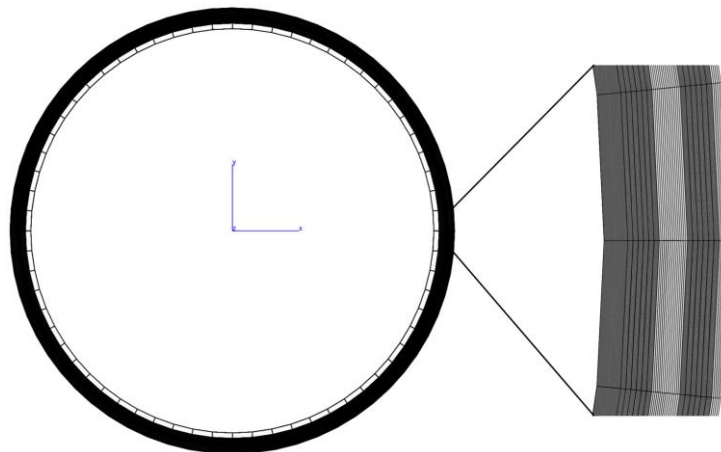


Figure 4. Mesh configuration of the ring geometry

Two types of geometries have been used in this study, the ring and CPV geometries. It was motivated by the idea of understanding the simulation approach that must be followed specifically for studying composite pressure vessels. The difference on the CPV simulation was the inclusion the tube and the dome geometries. The same ring geometry was then inserted in the middle of the tube as can be seen in

Fig. 5. The study has been conducted with different loading rates as performed experimentally. For each loading rate, 5 CPVs have been tested to failure. The same number of Monte-Carlo runs were performed for the ring simulations, whilst for the CPV simulation only one was carried out. The average value of the burst pressure could then be compared as shown in Fig. 8.

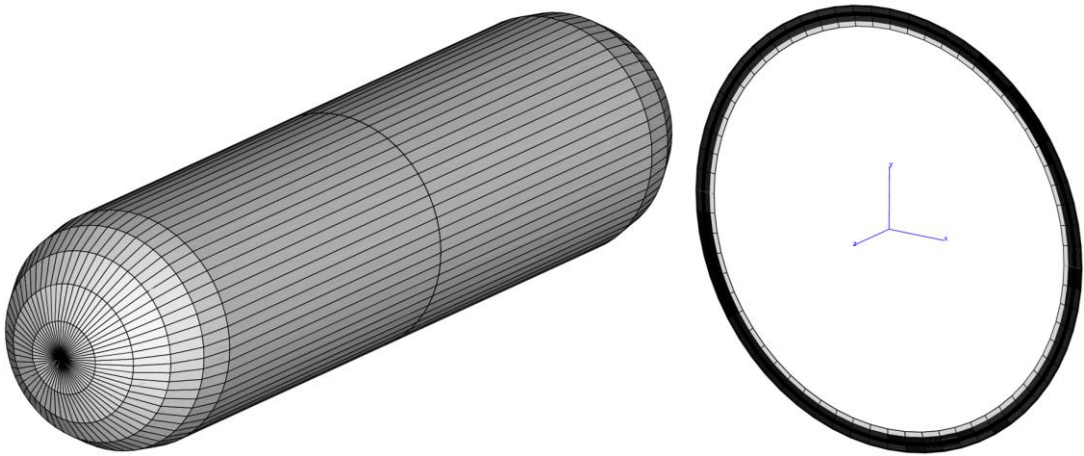


Figure 5. Mesh configuration of the cylinder geometry

3.0 BURST PRESSURE DETERMINATION

3.1 Graphical Solution

This can be done by looking at the number of fibre break results from the graphical user interface (GUI). The understanding is that the failure shall occur when all elements at which the fibre break model has been assigned to, reached the maximum 32-plets damage mode and eventually broke the studied structure into two separate parts, as shown in Fig. 6. This result then can be used to validate the average of the burst pressure values but not the scatter in the results. It is because that the graphical method does not include the effect of the accumulation of the fibres break which will affect the prediction of failure.

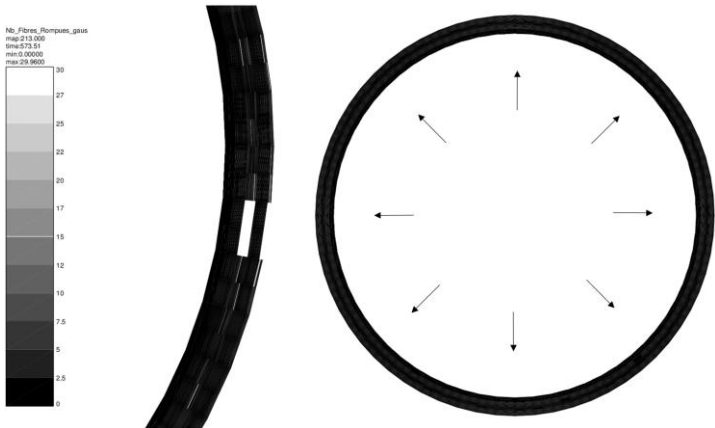


Figure 6. Graphical determination of the failure in ring simulation

The black colour represents the undamaged elements, whilst white means that the elements has been destroyed. The fibre break model has been deployed only for the hoop layers, hence the partial destruction of the angular section. The burst pressure had been calculated when the first angular section was found to be completely damaged.

3.2 Instability Technique

Composite structures often break quite suddenly, therefore it is not easy to predict when the structure will fail. The technique to capture this sudden moment can be examined with the model and it is referred as the instability technique. The data set for capturing the instability point was the accumulation of fibre breaks as a function of applied pressure. This has been chosen because the fibre break model has not been applied to the entire structure, so this data set was an accurate description of the modelled structures. Moreover, with this data set, the effect of the accumulation of fibre break for strength prediction could be included, unlike the previous method.

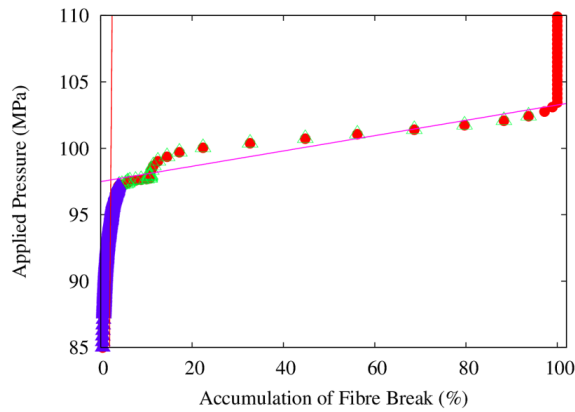


Figure 7. Determination of failure by including the effect of the accumulation of fibre break

Fig. 7 explained the accumulation of fibre break in the function of the applied pressure. The figure has been expanded in so that the accumulation process can be seen. The purple data set represents the data points from the beginning of the simulation until the point where the highest damaged-plets (32 plets) started to develop. From this point until the end of the loading process could be referred as the instability region. A linear regression of these two regions then would intersect at a point, which was the instability point. This point then could be understood as the burst pressure from the multiscale model.

Table 3. Comparison of failure stress between graphical and instability methods

Simulations	Burst Pressure (MPa)	
	Graphics	Instability
1	97.580	97.668
2	96.582	96.440
3	95.585	96.387
4	96.950	97.130
5	97.422	97.620
Average	96.824	97.049
Std. Deviation	0.650	0.504

The table above has confirmed that the prediction of burst pressure could be made by evaluating the accumulation of fibre breaks in the function of the applied pressure. Therefore, this technique now can be used with lower uncertainty to predict the burst pressure using the multiscale model.

4.0 RESULTS

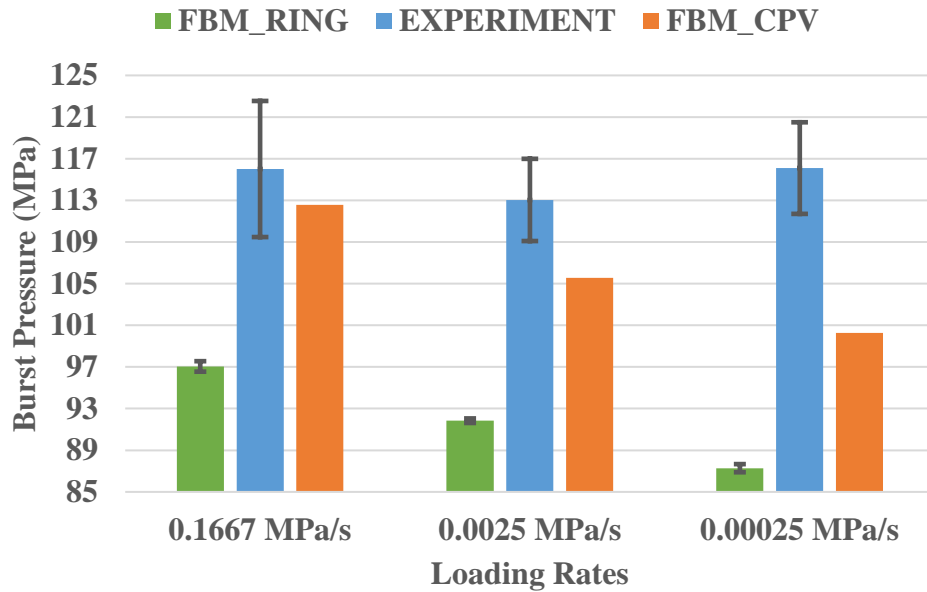


Figure 8. Comparison of the failure stress between the simulations and experimental results

Fig. 8 has shown that the multiscale model is able to show the time-dependent effect caused by the stress relaxation from broken fibres to the nearby intact fibres transferred via the shear stress of the matrix. It appeared that the cylinder simulations gave better predictions than the ring simulation. This was because of the force balance between the dome and the tube section of the ring, which could also be referred to the “*bottom effect*” that was not present in the ring simulation. This showed the importance of the 3D stress field that is required for the multiscale model to predict the failure stress accurately. The experimental result however showed that at the slowest loading rate, the average burst pressure value was similar to the one subjected with the fastest loading rate. This suggested that the accumulation process of fibre break at the slowest loading rate had been delayed as the rate was much slower than the rate of the stress relaxation in the matrix. This could allow the distribution of damages to occur in much larger volume in the cylinders, therefore as the loading continued with this rate, there would be more time for the load propagating to the existing damage, hence the similar results. If this were true, then each matrix property would have its own dependency to the applied loading rate, hence different process for evaluating the residual lifetime of CPV should be used. It should also be noted that as the speed was increased this approximated value more closely to an elastic situation in which the viscoelastic nature of the matrix was damped.

5.0 CONCLUSIONS

The study has explained the effect of the time-dependent load on a type IV pressure vessel. The model has shown that the CPV are more susceptible to the accumulation of damage when it is subjected with lower loading rate. It is important to mention that the difference in the material properties used in the simulation will affect the accumulation process of the fibre break, hence the difference in the reduction rate of burst pressures. Obtaining the accurate material properties sometimes is hindered due to confidentiality issues, nevertheless, the model has allowed the study of the accumulation of fibre break in CPV to be conducted. The determination of the scatter in the predictions still requires further study, as the relation of the statistical result from the reduced volume method study could be applied to the prediction of failure. In the end, the multiscale model works quite well for predicting the burst pressure at the highest loading rate.

6.0 DISCUSSIONS

It is important to be understood that the ring simulation had neglected the effect of the longitudinal stresses, which was introduced by the force balance between the dome and the tube region of cylinder geometries. This could also be explained with the comparison of the liner displacement between the ring and cylinder simulations as shown in Fig. 9. These data points represent the liner displacement of a node located in the X-axis (Z is the axial axis of the ring or CPV). Notice that the green data points behaved erratically and did give a negative displacement value at certain points. This indicated that every time an angular section accumulated more damage, the ring would give unrealistic radial displacement and became less rigid, see figure below. It would regain stability after all the elements in the hoop layer have been broken, which can be seen in the last stage of the curve. This phenomenon did not occur during the simulation of a cylinder, as can be seen from the linear increase of its liner displacement. This understanding has shown that the longitudinal stress plays a major role affecting the accumulation process of the fibre breaks, thus giving better predictions of the burst pressure.

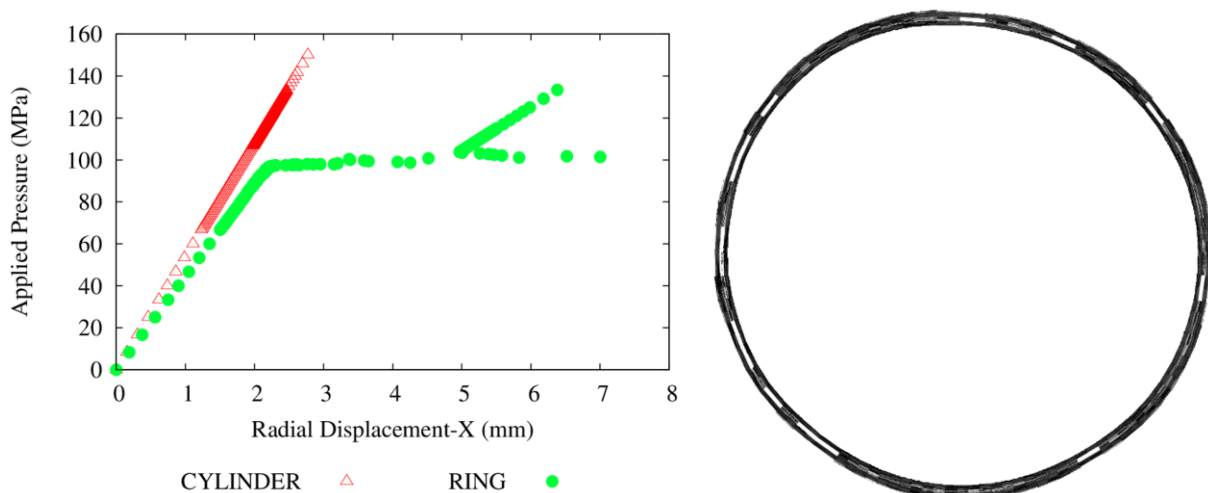


Figure 9. The displacement of liner in the function of applied pressure

ACKNOWLEDGEMENTS

The research leading to these results has been done within the framework of the FiBreMoD project and has received funding from the European Union's Horizon 2020 research and innovation programme under the Marie Skłodowska-Curie grant agreement No 722626.

REFERENCES

1. ISO 11119-3:2002 (E), Gas Cylinders of Composite Construction - Specification and Test Methods - Part 3: Fully Wrapped Fibre Reinforced Composite Gas Cylinders with Non-Load-Sharing Metallic or Non-Metallic Liners.
2. Becker, B. and Mair, G., Statistical Analysis of Burst Requirements from Regulations for Composite Cylinders in Hydrogen Transport, *Materials Testing*, **59**, 2017, pp. 226-232.
3. Bundesanstalt für Materialforschung und -prüfung (BAM), BAM-GGR 021, UN-Service Life Test Programme / Design Type Specific Determination of The Safe Service Life for Composite Pressure Receptacles on the Basis of the Concept Additional Tests (CAT), Berlin: Referenced in ISO TR 19811 / 5.3 Requirements as Approach no. 2, 2017.
4. Chou, H.Y., Bunsell, A.R., Mair, G. and Thionnet A., Effect of the Loading Rate on Ultimate Strength of Composites. Application: Pressure Vessel Slow Burst Test, *Composite Structures*, **104**, 2013, pp. 144-153.

5. Blassiau, S., Modelisation des Phenomenes Microstructuraux au sein d'un Composite Unidirectionnel Carbone/Epoxy et Prediction de Duree de Vie : Controle et Qualification de Reservoirs Bobines, Doctoral Thesis, Ecole de Mines ParisTech, France, 2005.
6. Widjaja, M.P., Joannes, S., Bunsell, A., Mair, G. and Thionnet, A., The Application of a Reduced Volume Method for the Simulation of the Characterisation of a Carbon Fibre Pressure Vessel, Proceedings of the 18th European Conference on Composite Materials (ECCM), 24-28 June 2018, Athens, in print.
7. Widjaja, M.P., Joannes, S., Bunsell, A., Mair, G. and Thionnet, A., Defining a Reduced Volume Zone for the Simulation of Burst Test on a Composite Pressure Vessel, Proceedings of the 8th International Conference on Structural Analysis of Advanced Materials (ICSAAM), 28-31 August 2018, Tarbes, in print.
8. Kratmann, K.K., Sutcliffe, M.P.F., Lilleheden, L.T., Pyrz, R. and Thomsen, O.T., A Novel Image Analysis Procedure for Measuring Fibre Misalignment in Unidirectional Fibre Composites, *Composite Science and Technology*, **69**, 2009, pp. 228-238.
9. Scott, A.E., Sinclair, I., Spearing, S.M., Thionnet, A. and Bunsell, A., Damage Accumulation in a Carbon/epoxy Composite: Comparison between a Multiscale Model and Computed Tomography Experimental Results, *Composites: Part A*, **43**, 2012, pp. 1514-1522.
10. Deng, S., Ye, L., Mai, Y. and Liu, H., Evaluation of Fibre Tensile Strength and Fibre/matrix Adhesion Using Single Fibre Fragmentation Tests, *Composites: Part A*, **29**, 1998, pp. 423-434.
11. Blassiau, S., Thionnet, A. and Bunsell, A., Micromechanisms of Load Transfer in a Unidirectional Carbon Fibre-Reinforced Epoxy Composite due to Fibre Failures: Part 3. Multiscale Reconstruction of Composite Behaviour, *Composite Structures*, **83**, 2008, pp. 312-323.
12. Blassiau, S., Thionnet, A. and Bunsell, A., Micromechanisms of Load Transfer in a Unidirectional Carbon Fibre-Reinforced Epoxy Composite due to Fibre Failures. Part 2: Influence of Viscoelastic and Plastic Matrices on the Mechanisms of Load Transfer, *Composite Structures*, **74**, 2006, pp. 319-331.
13. Blassiau, S., Thionnet, A. and Bunsell, A., Micromechanisms of Load Transfer in a Unidirectional Carbon Fibre-Reinforced Epoxy Composite due to Fibre Failures. Part 1 : Micromechanisms and 3D Analysis of Load Transfer: The Elastic Case, *Composite Structures*, **74**, 2006, pp. 303-318.
14. Blassiau, S., Thionnet, A. and Bunsell, A., Three-dimensional Analysis of Load Transfer Micromechanisms in Fibre/matrix Composites, *Composite Science and Technology*, **69**, 2009, pp. 33-39.
15. Thionnet, A., Chou, H.Y. and Bunsell, A., Fibre Break Processes in Unidirectional Composites, *Composites: Part A*, **65**, 2014, pp. 148-160.
16. Lantuejoul, C., Ergodicity and Integral Range, *Journal of Microscopy*, **161**, 1991, pp. 387-403.
17. Jeulin, D., Kanit, T. and Forest, S., Representative Volume Element : A statistical point of view, 2004, Kluwer Academic Publishers, Netherlands.
18. Dirrenberger, J., Forest, S. and Jeulin, D., Towards Gigantic Rve Sizes for 3D Stochastic Fibrous Networks, *International Journal of Solids and Structures*, **51**, 2014, pp. 359-376.
19. Easwaran, P., Hahn, F., Lehmann, M., Redenbach, C. and Schladitz, K., Representative Domain Size Study on Simulated 3d Fiber Systems, Proceedings of the Filtech exhibition, 11-13 October 2016, Cologne, in print.